rather a *CDKN2A* deletion was found in imatinib-insensitive areas after prior imatinib treatment. The relationship between a *CDKN2A* deletion and imatinib resistance has not been reported in GISTs but has been reported in Ph+ ALL.[5,6] The rapid proliferation of a leukaemic clone was suggested as a mechanism for *CDKN2A* deletion based on the imatinib resistance.[5] In GIST, mutations of *CDKN2A* have not been reported.[9] However, deletion of chromosome 9p arms harbouring *CDKN2A/B* loci have been identified by array comparative genomic hybridisation in 10% of GISTs as a predictive marker of recurrence or metastasis.[10] To find the frequencies of *CDKN2A* deletions in GIST, we searched all the NGS cancer panel test results performed in our institute. For the last 2 years, the NGS test has been performed in 19 patients with metastatic GIST treated with imatinib and showed evidence of progress of disease. Among them, three cases (15.7%) showed *CDKN2A* deletions. In the previous NGS study with 83 primary untreated GISTs, *CDKN2A* deletion was not reported.[9]

Based on these observations and our three cases having both *KIT* mutations and *CDKN2A* deletions, and showing progress of disease after imatinib treatment, *CDKN2A* deletions would lead to proliferation of mutant clones and cause those tumour cells insensitive to imatinib in GISTs.

Conflicts of interest and sources of funding: The authors state that there are no conflicts of interest to disclose.

Binnari Kim[1], Sang Yun Ha[1], Sujin Lee[2], Kyoung-Mee Kim[1]

[1]Department of Pathology and Translational Genomics, Samsung Medical Center, Sungkyunkwan University School of Medicine, Seoul, Republic of Korea; [2]Division of Hematology-Oncology, Department of Medicine, Samsung Medical Center, Sungkyunkwan University School of Medicine, Seoul, Republic of Korea

Contact Dr Kyoung-Mee Kim.
E-mail: kkmkys@skku.edu

1. Heinrich MC, Corless CL, Demetri GD, *et al*. Kinase mutations and imatinib response in patients with metastatic gastrointestinal stromal tumor. *J Clin Oncol* 2003; 21: 4342–9.
2. Quek R, George S. Update on the treatment of gastrointestinal stromal tumors (GISTs): role of imatinib. *Biologics* 2010; 4: 19–31.
3. Comandone A, Boglione A. The importance of mutational status in prognosis and therapy of GIST. *Recenti Prog Med* 2015; 106: 17–22 (Italian).
4. Sleijfer S, Wiemer E, Seynaeve C, *et al*. Improved insight into resistance mechanisms to imatinib in gastrointestinal stromal tumors: a basis for novel approaches and individualization of treatment. *Oncologist* 2007; 12: 719–26.
5. Mullighan CG, Williams RT, Downing JR, *et al*. Failure of CDKN2A/B (INK4A/B-ARF)-mediated tumor suppression and resistance to targeted therapy in acute lymphoblastic leukemia induced by BCR-ABL. *Genes Dev* 2008; 22: 1411–5.
6. Xu N, Li YL, Li X, *et al*. Correlation between deletion of the CDKN2 gene and tyrosine kinase inhibitor resistance in adult Philadelphia chromosome-positive acute lymphoblastic leukemia. *J Hematol Oncol* 2016; 9: 40.
7. Wang CM, Huang K, Zhou Y, *et al*. Molecular mechanisms of secondary imatinib resistance in patients with gastrointestinal stromal tumors. *J Cancer Res Clin Oncol* 2010; 136: 1065–71.
8. Kee D, Zalcberg JR. Current and emerging strategies for the management of imatinib-refractory advanced gastrointestinal stromal tumors. *Ther Adv Med Oncol* 2012; 4: 255–70.
9. Merten L, Agaimy A, Moskalev EA, *et al*. Inactivating mutations of RB1 and TP53 correlate with sarcomatous histomorphology and metastasis/recurrence in gastrointestinal stromal tumors. *Am J Clin Pathol* 2016; 146: 718–26.
10. Lagarde P, Perot G, Kauffmann A, *et al*. Mitotic checkpoints and chromosome instability are strong predictors of clinical outcome in gastrointestinal stromal tumors. *Clin Cancer Res* 2012; 18: 826–38.

DOI: https://doi.org/10.1016/j.pathol.2019.01.013

A novel case of linear IgG4-antibody mediated tubulointerstitial nephritis with concomitant HLA-B7, ANCA-MPO

Sir,

IgG4-related disease (IgG4-RD) is a usually systemic disease with raised serum IgG4, and when the kidney is involved there is abundant IgG4 positive plasma cells infiltration with a storiform interstitial fibrosis.[1] The anti-neutrophil cytoplasmic antibodies (ANCAs), most commonly myeloperoxidase (MPO) and proteinase 3 (PR3), are usually associated with pauci-immune systemic vasculitis and crescentic glomerulonephritis (Cr GN). The occurrence of double MPO-ANCA and anti-glomerular basement membrane antibody nephritis (anti-GBM-Ab nephritis) with linear IgG, C3 along the GBM are uncommon, and known to occur in only 0.73% (10) of 1,373 cases of crescentic GN.[2] Only 10 cases have been identified in the literature of IgG4-RD and ANCA-associated vasculitis. A rare case of concomitant IgG4-RD tubulointerstitial nephritis with pauci-immune IgG4-MPO-ANCA with necrotising crescentic GN with C3 and fibrinogen has been reported.[3] We report a novel case of a young adult male with IgG4 tubulointerstitial nephritis (IgG4-TIN) with no necrotising crescentic nephritis, with linear IgG4 along the tubular basement membrane (TBM), and with concomitant HLA-B7 and persistently elevated ANCA-MPO, and with no GBM involvement by immunoglobulins or complements. There was rapidly progressive renal failure treated by plasma exchange (PEX) and immunosuppression.

A 23-year-old Caucasian male was referred in April 2015 with past history of correction of transposition of great arteries at the age of two. Serum creatinine was 146 µmol/L, eGFR 58 mL/min/1.73 m^2, positive (MPO) ANCA 15 U/mL (normal <3.5 U/mL), and bland urine sediment with normal urine albumin creatinine ratio (uACR). Ultrasound showed normal renal cortico-medullary differentiation. In January 2016, renal function declined with eGFR 44 mL/min/1.73 m^2. Percutaneous renal biopsies were performed for diagnosis and follow up. Renal core biopsies were placed in 10% buffered formalin for light microscopy, in optimal cutting temperature (OCT) compound then snap frozen in liquid nitrogen for immunofluorescence microscopy, or in 2.5% glutaraldehyde for electron microscopy. For light microscopy, fixed tissues were routinely processed, paraffin-embedded and 2 µm sections were stained with haematoxylin and eosin (H&E), periodic acid-Schiff (PAS), periodic acid methenamine silver (PAMS) or modified Mallory's trichrome. Sections were also examined by immunohistochemistry using antibodies against cell markers of T and B cells, macrophages and plasma cells, CD3 (clone2GV6),

CD4 (SP35), CD8 (SP57), CD20 (L26), CD138 (B-A38), CD163 (MRQ-26) (Ventana, USA) and IgG4 (HP6025; Invitrogen, USA). The tests were performed on a Ventana Benchmark Ultra platform using routine protocols and Ventana detection kits. Snap frozen tissue was stored at −80°C prior to cutting 5 µm sections and staining for 30 min with the following fluorescein isothiocyanate (FITC) conjugated antibodies: polyclonal IgA, IgG, IgM, C3c, C4c, C1q, fibrinogen, kappa and lambda light chains (Dako, Denmark) and monoclonal IgG1 and IgG4 (Sigma, USA). IgA, IgM, C3c, C4c and C1q antibodies were used at 1:40 dilution; the remaining antibodies were used at 1:50 dilution. Immunostained slides were viewed using a Leica DM2500 microscope (Leica, Germany) using the appropriate fluorescence filter cube.

The first biopsy for diagnosis showed focal mild interstitial inflammation, fibrosis, tubular atrophy and focal periglomerular fibrosis and glomerulosclerosis. The patient was lost to follow-up until 13 months later, in May 2017, when serum creatinine was 494 µmol/L, eGFR 13 mL/min/1.73 m^2. Urinalysis remained negative for microscopic haematuria but there was mild proteinuria (0.5 g/day), glycosuria with random normal plasma glucose (4.6 mmol/L). MPO-ANCA titre remained unchanged at 9.7 U/mL. The pre-treatment serum IgG was mildly raised 13.4 g/L (normal 6.1−13.0 g/L); IgG subtyping showed normal IgG1 8.18 g/L (4.90−11.40 g/L), and raised IgG4 1.86 (0.08−1.40). An updated ultrasound demonstrated bilateral cortical thinning. A second renal biopsy was undertaken, demonstrating significant progression since the first biopsy 18 months previously. In light of the diagnosis of anti-TBM-Ab-TIN, he was commenced on oral prednisolone 50 mg. Simultaneous PEX were undertaken, with a total of six sessions of PEX over a period of 2 weeks. Prednisolone was gradually weaned over a period of 9 months. Renal function continued to deteriorate over this time frame. Serum creatinine levels hovered between 550 and 600 µmol/L by March 2018. HLA-typing revealed the following alleles: A (2,3), B (7,27), C (2,7), DRB1 (12,13) and DRB3 (2,3).

The first kidney biopsy performed in January 2016 contained two cores of renal cortex, each with >20 glomeruli. One core was essentially normal except for foci of mild interstitial inflammation, mainly lymphocytes, a small number of plasma cells and neutrophils, and no interstitial fibrosis or glomerulosclerosis. The glomeruli showed no inflammatory cells or necrotising crescentic nephritis or glomerulosclerosis (Fig. 1A). The second core showed a segmental zone of interstitial fibrosis, and in this area six of 19 glomeruli showed only periglomerular fibrosis and no glomerulitis or necrotising crescentic lesions. There was tubular atrophy, moderate chronic inflammatory cells infiltration, mainly small lymphocytes and plasma cells, a small number of neutrophils and few lymphoid nodules. The interlobular arteries and arterioles showed no vasculitis or significant arteriosclerosis (Fig. 1B). There was approximately <20% renal parenchymal damage of the combined two cores of renal tissue. The second kidney biopsy taken 18 months later (June 2017) showed progression to severe interstitial fibrosis, tubular atrophy and 66% (20/30) ischaemic type glomerulosclerosis, and periglomerular fibrosis, without glomerulosclerosis in most of the other glomeruli. There was moderate to severe interstitial inflammation, predominantly small lymphocytes, macrophages and plasma cells mainly in the scarred areas with a storiform fibrosis. The blood vessels showed moderate arterial sclerosis and no vasculitis (Fig. 1C). There was progressive severe interstitial fibrosis and inflammation over the 18 month period, with >90% chronic parenchymal damage. Direct immunofluorescence microscopy showed bright linear binding of polyclonal IgG (3+), monoclonal IgG4 (3+), C3c (3+), kappa (3+) and lambda (3+) light chains along the tubular basement membrane both on normal and atrophic tubules, and also on Bowman capsule (Fig. 1D,E). There was negative staining for IgG1, IgA, IgM, C4c and C1q. There was no binding of immunoglobulins or complements along the GBM or the mesangium.

At 18 months there was severe inflammation and fibrosis with a polymorphic inflammatory cells infiltration of B cells (CD20) (Fig. 1F) and T cells (CD3), ratio CD20:CD3 = 2:1, CD163+ macrophages and small population CD138+ plasma cells. There was a greater number of CD4+ T helper cells (Fig. 1G) to CD8+ suppressor cells, ratio CD4:CD8 = 20:1. The immunoperoxidase stains showed the greatest concentration of IgG4+ plasma cells in the scarred areas, with >50 IgG4+ plasma cells per HPF (×40) in the first biopsy, and >70 IgG4+ plasma cells per HPF (×40) (Fig. 1H) in the second biopsy, with the most density in areas of fibrosis. Linear IgG4 deposits were seen on the TBM of both normal and abnormal zones of the kidney and involved both the proximal and distal tubules. No deposits were seen in the glomeruli.

As serum anti-TBM Ab was not commercially available, the following investigations were performed to identify anti-TBM antibodies in the patient's serum. Indirect immunofluorescence microscopy was performed with serum from the patient serving as a primary antibody, followed by FITC-conjugated IgG4 as secondary label antibody for the detection of the endogenous TBM antigen. The titre of circulating anti-TBM-Ab was assessed with whole serum, and serial dilutions neat, 1:10 and 1:20 dilutions. As negative control, serum from a kidney donor with blood group AB and with no preformed antibodies was used. The patient's serum and the control serum from blood group AB were tested on the tissues of ten normal human kidneys obtained from kidney donors with no preformed antibodies and no immunoglobulin or complement deposits in the glomeruli or tubulointerstitium. Three pre-treatment and seven post-PEX serum samples varying from 2 weeks to 10 months were examined. Three pre-PEX sera tagged with FITC-conjugated polyclonal IgG, monoclonal IgG4 and IgG1, and at dilutions neat, 1:10, and 1:20, showed strong linear IgG (3+) and IgG4 (3+) along the TBM in the ten negative control donor kidneys at dilutions neat and 1:10 (Fig. 2A) and weak (1+) at 1:20. Monoclonal IgG1 was negative. The negative control AB serum showed negative staining in the control donor kidneys (Fig. 2B). All the tests showed negative staining of the GBM and mesangium. The seven post-PEX sera from the patient taken from 2 weeks to 10 months were tested. They showed no staining of the TBM, Bowman capsule or GBM; however, the 6 month post-PEX serum showed mild (1+) to moderate (2+) linear staining of IgG and IgG4, and negative IgG1, along the TBM and not the GBM or mesangium of the control normal kidneys. The serum from the 8th month PEX showed moderate (2+) linear staining for IgG4 (2+) at dilution neat, and by the 10th month prePEX levels intensity of IgG4 (3+) neat, and IgG4 (1−2+) at dilution 1:10 were present (Fig. 2C). All 10

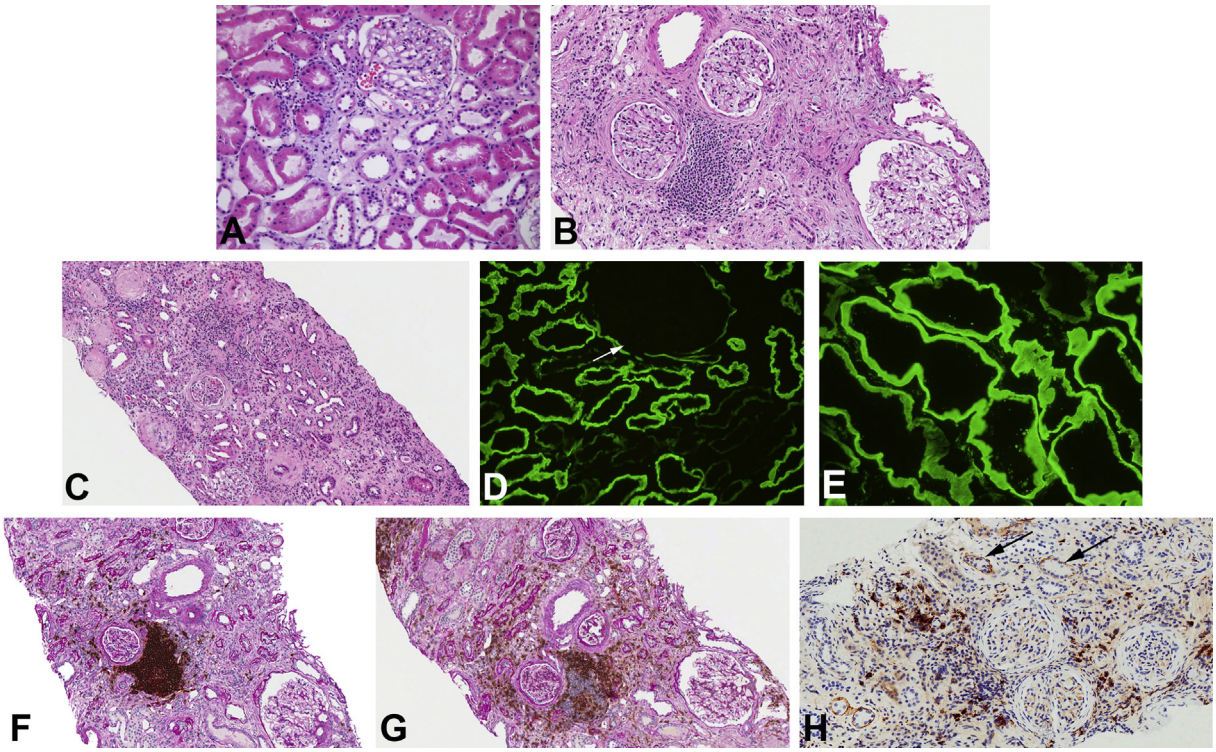

Fig. 1 (A,B) First renal biopsy. There are two distinct zones: (A) one core is nearly normal; (B) a second piece shows a segmental zone of interstitial fibrosis and inflammation. (C−E) Second renal biopsy taken 18 months later shows severe interstitial fibrosis, tubular atrophy and inflammatory cells infiltration. The mononuclear cells are mainly lymphocytes and a moderate number of plasma cells. (C) There is now extensive global glomerular sclerosis (H&E). (D) Direct immunofluorescence microscopy shows IgG4 (3+) bright linear staining of the tubular basement membrane (TBM) and Bowman capsule and negative staining of the glomerulus (arrows); (E) high power of the TBM IgG4 linear staining. (F) There are CD20+ B cells, (G) CD4+ T helper cells, and (H) >50 IgG4+ plasma cells per HPF, and linear IgG4 along the TBM.

normal control kidneys showed no significant immunoprotein or complement deposits. Electron microscopy (EM) examination of both kidney biopsies showed no electron dense or discrete deposits along the TBM or the GBM including the mesangium. There was no GBM abnormality or laminopathy, with a mean GBM thickness of 381 nm (SD±14) (Fig. 2D,E).

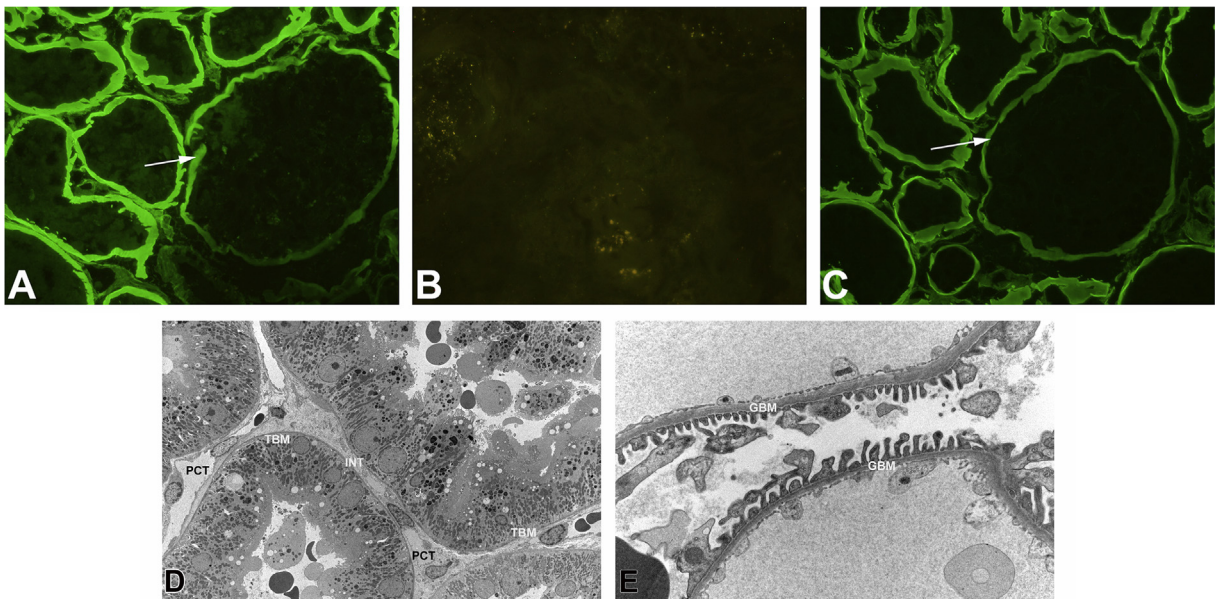

Fig. 2 Indirect immunofluorescence microscopy of the patient's pre-treatment serum as primary antibody and FITC-conjugated IgG4 as secondary antibodies on the control normal kidney shows bright linear staining for IgG4 along the tubular basement membrane (TBM) and Bowman capsule, at dilutions neat and 1:10. (A) There is no staining of the glomerulus (arrow). (B) The negative control AB serum with FITC-conjugated IgG4 as the secondary antibody showed no staining of the TBM or glomerulus in normal control kidneys. (C) The patient's serum at 8 months post-treatment on control normal kidneys showed re-appearance of the linear IgG4 (2+−3+), neat, along the tubular basement membrane and Bowman capsule, and negative in the glomerulus (arrow). (D) Electron microscopy of the patient's first renal biopsy. There are no dense discrete or amorphous deposits seen along the TBM, peritubular capillaries (PTC) or the interstitium (INT). (E) There are also no deposits along the glomerular basement membrane (GBM), both in the normal and damaged zones of the kidney.

The TBM Ag glycoprotein is the primary target of anti-TBM antibodies in human and experimental immunologically-mediated anti-TBM nephritis. It is a non-collagen glycoprotein of 40 kDa, major 58 kDa, 54 kDa and 48 kDa, and the antibodies elicit responses to type IV procollagen, and another group of antibodies resulting in response to non-collagenous glycocollagen present in the TBM only.[4] All show linear deposition of IgG along the TBM but not along the GBM. This is in contrast to the Goodpasture antigen which is localised to the collagen IV domain of GBM.[5]

Primary anti-TBM interstitial nephritis with linear IgG and C3c presents with acute renal failure usually in the young (27−36 years). In immune complex-mediated TIN IgG and C3 are granular and EM shows amorphous deposits in the TBM.[6] Secondary anti-TBM-Ab TIN include Fanconi's familial nephronophthisis, drug-induced TIN, renal allograft, Sjögren's syndrome, TIN with uveitis (TINU), and anti-TBM-Ab-TIN with membranous glomerulonephritis (MN).[7] The criteria for the diagnosis of IgG4-RD renal disease include >10 IgG4+ plasma cells per high power field (HPF) (magnification ×40) in the densest infiltrates; >30 IgG4+ cells per HPF (×40) are considered markedly increased, and the deposits are granular IgG4, often with C3c, and are discrete on EM.[8]

Our case shows linear deposition of predominantly IgG4 and C3c along the TBM and Bowman capsule, and no staining of the GBM. There is interstitial nephritis with reactive CD3+ T cells, CD4+ T helper cells > CD8+ T suppressor cells, CD163+ macrophages, CD20+ B cells and IgG4-plasmacytosis mainly in the areas of inflammation leading to progressive interstitial fibrosis. In our HLA-B7 patient with no glomerulitis or necrotising crescentic lesions, or vasculitis, the concomitant MPO-ANCA released by inflammatory cells could possibly expose the hidden TBM antigen and trigger an autoimmune response with linear IgG4, C3c TIN. A previous report also demonstrated a possible association of HLA-B7 and/or DRW8 to anti-TBM-TIN associated with MN in sera from three patients from two unrelated families.[7] Our patient does not have MN and has never developed significant proteinuria. Nonetheless, the presence of B7 allele may pose increased susceptibility to the development of IgG4-RD-TIN in young patients, as most patients with IgG4-TIN-RD are reported to be in their sixties. Anti-plasminogen antibodies were detected in approximately 25% patients in both PR3-ANCA and MPO-ANCA and had a significantly higher percentage of glomeruli with fibrinoid necrosis and cellular crescents,[9] lesions which were not seen in our patient. In our case, anti-TBM-Ab-mediated TIN with linear IgG4, IgG and C3c along the TBM and Bowman capsule only, with an interstitial nephritis with reactive CD3+ T cells, CD4+ T helper cells > CD8+ T suppressor cells, CD163+ macrophages, CD20+ B cells, IgG4-plasmacytosis and linear IgG4 deposits seen in both normal and in inflamed fibrotic zones, support the experimental studies of the immune response directed to a glycoprotein found along the tubules of the kidney.[10,11] The likely interaction of the T and B cells infiltrates leads to tubulointerstitial damage which occurs via the cognate B cell/T cell interaction. It also provides co-stimulation to B cells, which become activated via CD40 ligand expressed on T cells, and which provide cytokines to B cells that support their survival (IL-4), and differentiate into plasma cells (IL-21). CD4+ memory T cells may also play a pivotal role in humoral immunity.[12] These interactive mechanisms would explain the nephritogenic effect on the tubulointerstitium, and the plasmacytosis with humoral IgG4 expression. PEX was effective in removing circulating IgG4-antibodies, and later also ANCA-MPO which was within normal (0.3 μ/mL) in October 2018, and with negative IgG4 along the TBM of normal control kidney. However, on cessation of treatment there was rebound detectable by 6 months, and to pre-PEX levels by 10 months. The role of prednisolone and anti-CD20 monoclonal antibodies could not be evaluated as treatment was instituted rather late. Post-transplant management with regular PEX, monitoring of serum IgG4 and ANCA-MPO, and more accurately renal biopsy monitoring for linear IgG4 and C3c on normal control kidneys tested with patient serum and FITC-conjugated IgG4, is a reliable strategy.

In summary, our young male with HLA, B7 allele and concomitant MPO-ANCA, may have had increased susceptibility to the development of linear IgG4-anti-TBM-Ab-TIN, leading to rapidly progressive interstitial fibrosis. PEX is effective in removing the circulating antibodies and periodic testing of the patient's serum for linear IgG4 along the TBM on control kidneys should be the strategy for management of the patient post-transplant. Documentation of similar unique cases would assist in better understanding, early diagnosis and management of similar rare renal diseases.

Acknowledgements: We thank Dr L. D'Orsogna and Mr Nick Aquarola, Department of Immunology, Fiona Stanley Hospital, for providing the initial prePEX serum, and serum from the blood group AB patient; Ms Sallyanne Cousans and Mr Paul Scharf for the photography; Mr Pierre Filion for the electron microscopy; Mrs Carolyn Brown and Ms Rhondda Banfield for secretarial assistance; PathWest Laboratory Medicine.

Conflicts of interest and sources of funding: This work was carried out using the materials and facilities of PathWest Laboratory Medicine and Fiona Stanley Hospital. There were no financial or other relationships with pharmaceutical or commercial firms, and no conflicts of interest exist.

Rajalingam Sinniah[1,2,3], Terry Kop[1], George Chin[2]

[1]Department of Anatomic Pathology, PathWest Laboratory Medicine, Perth, WA, Australia; [2]Department of Nephrology, Fiona Stanley Hospital, Perth, WA, Australia; [3]University of Western Australia, Perth, WA, Australia

Contact Prof Rajalingam Sinniah.
E-mail: Rajalingam.Sinniah@health.wa.gov.au

1. Deshpande V, Zen Y, Chan JK, *et al*. Consensus statement on the pathology of IgG4-related disease. *Mod Pathol* 2012; 25: 1181−92.
2. Rutgers A, Slot M, van Paassen P, *et al*. Co-existence of anti-glomerular basement membrane antibodies and myeloperoxidase-ANCAs in crescentic glomerulonephritis. *Am J Kidney Dis* 2005; 46: 253−62.
3. Su T, Yang L, Cui Z, *et al*. Concurrent IgG4-related tubulointerstitial nephritis and IgG4 myeloperoxidase anti-neutrophil cytoplasmic antibody positive crescentic glomerulonephritis: a case report. *Medicine (Baltimore)* 2017; 96: e6707.
4. Wakashin Y, Takei I, Ueda S, *et al*. Autoimmune interstitial disease of the kidney and associated antigen purification and characterisation of a soluble tubular basement membrane antigen. *Clin Immunol Immunopathol* 1981; 19: 360−71.

5. Butkowski RJ, Wieslander J, Wisdom BJ, *et al*. Properties of the glomerular domain of type IV collagen and its relationship to the Goodpasture antigen. *J Biol Chem* 1985; 260: 3739–47.
6. Brentjens JR, Matsuo S, Fukatsu A. Immunologic studies in two patients with antitubular basement membrane nephritis. *Am J Med* 1989; 86: 603–8.
7. Katz A, Fish AJ, Santamaria P, *et al*. The role of antibodies to tubulointerstitial nephritis antigen in human anti-tubular basement membrane nephritis associated with membranous nephropathy. *Am J Med* 1992; 93: 691–8.
8. Salvadori M, Tsalouchos A. Immunoglobulin G4-related kidney diseases: an updated review. *World J Nephrol* 2018; 7: 29–40.
9. Berden AE, Nolan SL, Morris HL, *et al*. Anti-plasminogen antibodies compromise fibrinolysis and associate with renal histology in ANCA-associated vasculitis. *J Am Soc Nephrol* 2010; 21: 2169–79.
10. Mann RA, Zakhein B, Claymen MD, *et al*. Murine interstitial nephritis. IV. Long-term cultured L3T4 + T-cell lines transfer delayed expression of disease as 1-A restricted inducers of the effector T cell repertoire. *J Immunol* 1985; 135: 286–93.
11. Neilsen EG, Sun MJ, Kelly CJ, *et al*. Molecular characterisation of a major nephritogenic domain in the auto-antigen of anti-tubular basement membrane disease. *Proc Nat Acad Sci USA* 1991; 88: 2006–10.
12. International Union of Immunological Societies. Immunopaedia.org. Cited Nov 2018. https://immunopaedia.org/

DOI: https://doi.org/10.1016/j.pathol.2019.01.014

Epstein–Barr virus positive mucocutaneous ulcer of vulva

Sir,

Epstein–Barr virus positive mucocutaneous ulcer (EBV-MCU) is a recently recognised B cell lymphoproliferative disorder that is driven by latent EBV infection. The ulcer is described to occur in patients with age-related or iatrogenic immunosuppression, often with a Hodgkin-like pattern and an indolent course, including spontaneous regression.[1] In humans, EBV is the most common persistent virus infection, where it elicits the B-cell proliferation and transformation. The World Health Organization (WHO) 2017 discusses two lymphoproliferative diseases that are associated with EBV: EBV positive diffuse large B cell lymphoma and EBV-MCU. EBV-MCU is a rare provisional entity which is likely under-reported secondary to its recent recognition and morphological and immunophenotypical similarities to Hodgkin lymphoma. EBV-MCU occurs most commonly in the oropharynx, gastrointestinal tract and skin.[2] To the best of our knowledge there is no report in the English published literature of EBV-MCU presenting as a vulval introital ulcer.

Here we present a case of an EBV-MCU in a 78-year-old female, who presented with a vulval introital ulcer. She was a known case of rheumatoid arthritis on methotrexate (MTX) for 3 years, 20 mg per week. There was no history of trauma, or tobacco consumption. The clinical examination revealed a 4×4 cm introital ulcer in the midline. An excisional biopsy of the ulcer was performed. The histological examination revealed squamous mucosa with extensive ulceration (Fig. 1A). The underlying granulation tissue showed a moderate infiltrate of lymphoid cells admixed with a few scattered eosinophils (Fig. 1B). Many of the lymphoid cells showed atypia with enlarged 'blastic' appearing nuclei and clear cytoplasm. However, the infiltrate appeared polymorphous with zonation of the less mature appearing lymphoid cells in the superficial stroma. The atypical lymphoid cells were positive for CD20 (Fig. 1C), EBER (Fig. 1D), Bcl2, CD30, CD43, and CD15 and negative for CD3, CD10, bcl6, CD5, CD23, CD5 and CD4. In view of the history of MTX induced immunosuppression, histology, and supporting immunohistochemistry, a diagnosis consistent with EBV-MCU was made by two general surgical pathologists (SA, CSL) and a haematopathologist (CCCC).

Polymerase chain reaction (PCR) amplification for gene rearrangements of the IgH, Ig-kappa (IgK), TCR-beta (TCRB) and TCR-gamma (TCRG) (courtesy of Dr Benhur Amanuel, PathWest) showed monoclonal IgK rearrangement. Positron emission tomography (PET) scan and CT-scan performed 2 months following surgery showed no evidence of nodal or extranodal involvement by the lymphoproliferative disease. The patient was managed by reducing her immunosuppressant therapy for her rheumatoid arthritis and she remained free of the disease at follow-up 5 months following the initial diagnosis.

In 2010, Dojcinov *et al.*[3] first reported the entity EBV-MCU in 26 patients, nine associated with immunosuppression caused by MTX, azathioprine, and cyclosporine-A given for autoimmune diseases and 17 with ulceration of the skin or mucosa with no systemic involvement as evident in this case. In 2014, Hart *et al.*[4] reported seven patients of EBV-MCU in 70 solid organ transplant recipients with EBV positive post-transplant lymphoproliferative disorder (PTLD). In 2015, Bunn *et al.*[5] described two cases of AIDS-related EBV-MCU. Most EBV-MCU cases are self-limited, however a few reported cases have progressed or even transformed into classical Hodgkin lymphoma (CHL).[6] In the latter cases, it is unclear whether EBV-MCU might be a precursor of CHL or the initial diagnosis was actually EBV positive CHL with overlapping features with EBV-MCU. The spectrum of age-related, EBV positive lymphoproliferative disorders (aEBVLPD) was first described by Oyama and co-workers and distinctively occurs in elderly patients without any history of immunosuppression.[7]

EBV has long been associated with B-cell lymphoproliferative disorders. After primary infection at an early age EBV persistently infects B cells of most adults. The virus elicits B-cell transformation and proliferation through complex mechanisms. The viral genes upregulate a variety of cellular antigens and expression of genes in B cells. Key molecular pathways controlling the cell cycle, such as nuclear factor kappa-light-chain-enhancer of activated B cells (NF-κB), are activated and virus-induced cytokines exert paracrine proliferative effects.[8] The pathological features are identical regardless of the anatomical site or cause of immunosuppression. Histologically, EBV-MCU is characterised by a polymorphous infiltrate and atypical large B cells with Hodgkin/Reed Sternberg (HRS) cell-like morphology and admixed abundant T cells. Angioinvasion and necrosis can be present in addition to surface ulceration. The large B cells are consistently positive for EBV by latent membrane protein (LMP) and *in situ* hybridisation. About one-third of cases are clonal for immunoglobulin receptor gene or T-cell receptor gene rearrangement. These pathological, immunophenotypical, and molecular features might overlap with lymphoma.[9]

In summary, EBV-MCU must be distinguished from the more aggressive systemic PTLD and lymphomas, especially CHL, EBV positive diffuse large B-cell lymphoma, plasmablastic lymphoma, and anaplastic large cell lymphoma. A